

LETTER • OPEN ACCESS

Persistent anticyclonic conditions and climate change exacerbated the exceptional 2022 European-Mediterranean drought

To cite this article: Davide Faranda *et al* 2023 *Environ. Res. Lett.* **18** 034030

View the [article online](#) for updates and enhancements.

You may also like

- [ZOMBIE VORTEX INSTABILITY. II. THRESHOLDS TO TRIGGER INSTABILITY AND THE PROPERTIES OF ZOMBIE TURBULENCE IN THE DEAD ZONES OF PROTOPLANETARY DISKS](#)

Philip S. Marcus, Suyang Pei, Chung-Hsiang Jiang *et al.*

- [Large-scale Vortices in Rapidly Rotating Rayleigh–Bénard Convection at Small Prandtl number](#)

Tao Cai

- [The Streaming Instability in Two-dimensional Protoplanetary Disks](#)

Liubin Pan and Cong Yu



Breath Biopsy® OMNI®

The most advanced, complete solution for global breath biomarker analysis

TRANSFORM YOUR RESEARCH WORKFLOW



Expert Study Design & Management



Robust Breath Collection



Reliable Sample Processing & Analysis



In-depth Data Analysis



Specialist Data Interpretation

ENVIRONMENTAL RESEARCH
LETTERS

LETTER

Persistent anticyclonic conditions and climate change exacerbated the exceptional 2022 European-Mediterranean drought

OPEN ACCESS

RECEIVED
20 December 2022REVISED
27 January 2023ACCEPTED FOR PUBLICATION
15 February 2023PUBLISHED
28 February 2023

Original Content from this work may be used under the terms of the [Creative Commons Attribution 4.0 licence](https://creativecommons.org/licenses/by/4.0/).

Any further distribution of this work must maintain attribution to the author(s) and the title of the work, journal citation and DOI.

Davide Faranda^{1,2,3,6,*} , Salvatore Pascale^{4,5,6}  and Burak Bulut^{1,6} 

¹ Laboratoire des Sciences du Climat et de l'Environnement, UMR 8212 CEA-CNRS-UVSQ, Université Paris-Saclay & IPSL, CE Saclay l'Orme des Merisiers, 91191 Gif-sur-Yvette, France

² London Mathematical Laboratory, 8 Margravine Gardens, London W6 8RH, British Islands

³ Laboratoire de Météorologie Dynamique/IPSL, École Normale Supérieure, PSL Research University, Sorbonne Université, École Polytechnique, IP Paris, CNRS, 75005 Paris, France

⁴ University of Bologna, Department of Physics and Astronomy, 40126 Bologna, Italy

⁵ Centre for Sustainability and Climate Change, Bologna Business School, 40136 Bologna, Italy

⁶ All authors have equally contributed to this work.

* Author to whom any correspondence should be addressed.

E-mail: davide.faranda@cea.fr

Keywords: drought, climate change, attribution

Supplementary material for this article is available [online](#)

Abstract

A prolonged drought affected Western Europe and the Mediterranean region in 2022 producing large socio-ecological impacts. The role of anthropogenic climate change (ACC) in exacerbating this drought has been often invoked in the public debate, but the link between atmospheric circulation and ACC has not received much attention so far. Here we address this question by applying the method of circulation analogs, which allows us to identify atmospheric patterns in the period 1836–2021 very similar to those occurred in 2022. By comparing the circulation analogs when global warming was absent (1836–1915) with those occurred recently (1942–2021), and by excluding interannual and interdecadal variability as possible drivers, we identify the contribution of ACC. The 2022 drought was associated with a persistent anticyclonic anomaly over Western Europe. Circulation analogs of this atmospheric pattern in 1941–2021 feature 500 hPa geopotential height anomalies larger in both extent and magnitude, and higher temperatures at the surface, relative to those in 1836–1915. Both factors exacerbated the drought, by increasing the area affected and enhancing soil drying through evapotranspiration. While the occurrence of the atmospheric circulation associated with the 2022 drought has not become more frequent in recent decades, the influence of the Atlantic Multidecadal oscillation cannot be ruled-out.

1. Characteristics of the 2022 Euro-Mediterranean drought

Intense and prolonged drought conditions affected large portions of France, Italy, and Spain throughout most of 2022. The drought, related to a persistent lack of precipitation in the last months of 2021, became evident in northwestern Italy since March 2022 [1] and then expanded to western Europe in the following months. The severity of the drought then further worsened during spring and summer 2022 (figure 1(b)), due to a persistent

lack of precipitation combined with a sequence of heatwaves from May onwards [2, 3] which further dried the soil through enhanced evapotranspiration [4]. Using the Standardized Precipitation Evapotranspiration Index aggregated at nine months (SPEI9) to monitor and characterize the 2022 drought [4, 5], we show in figure 1(c) and (d) the record-breaking negative values of the drought indicator SPEI9 in August 2022 (see section 2.1 for details about SPEI) over southern France and Northern Italy. The area-average of SPEI9 over the two areas was consistently below -2 (extreme

drought), with local grid points having SPEI9 values below -3 .

The socio-ecological impacts of the 2022 drought have been severe in Italy, France and Spain. The exceptionality of the water and heat stress substantially reduced yields of some of the main crops like, e.g. grain maize, soybean, and sunflowers, with reductions of around 15% relative to the last 5-year average [6]. In Italy, about 50% of the population was affected by the drought emergency water restrictions, especially in the North of the country. The Po river basin Authority reported record-breaking levels of inland salt intrusion from the Po delta up to 40 km from the sea coast. Reduced stored water severely impacted the energy sector for both hydropower generation and cooling systems of other power plants in the north of the country. In southern France, wildfires associated with the extreme drought conditions were also more widespread, with a surface of burned land more than double than in 2021 and about 4.6 times the average of the period 2012–2021. Sixty-six French ‘departments’ were at the highest drought warning level in August, with at least ninety-three departments at one of the top three levels of warning for drought. Similar impacts on agriculture, energy production and domestic water usage were reported in Spain, Portugal and Netherlands too [2].

While drought is a complex phenomenon [7, 8], whose intensity can be exacerbated by non-trivial land surface-atmosphere feedbacks and land usage [9], the large scale atmospheric circulation played a key role in driving the 2022 Euro-Mediterranean drought. This is evident when examining the mean December 2021–August 2022 circulation anomalies: a persistent high pressure anomaly centered over France is visible both in the lower and middle troposphere (figure 1(a)). This circulation anomaly favored meteorological conditions characterized by stable conditions with no precipitation over large swaths of Europe.

The 2022 Euro-Mediterranean drought unfolded as El Niño-Southern Oscillation (ENSO) was in a persistent negative phase (La Niña) since the summer of 2020. It is therefore natural to ask whether La Niña did play a role in remotely driving the long-lasting anticyclonic circulation. The relationship between ENSO and the North Atlantic-European sector is not as well defined as for other regions of the world, and probably non-stationary in time [10–12]. If we compare the slow-evolving circulation anomaly of 2022 in Europe with that of other years featuring similar three-year La Niña conditions (i.e. 1956, 1975 and 2000), we see large differences in the intensity and spatial patterns of the anomalies and no resemblance to the 2022 pattern (figure S1). This leads us to conjecture that there might not be a simple causality relationship between La Niña and the persistent anticyclonic anomaly observed over western Europe in 2022,

although this is a point that we will further investigate in this study.

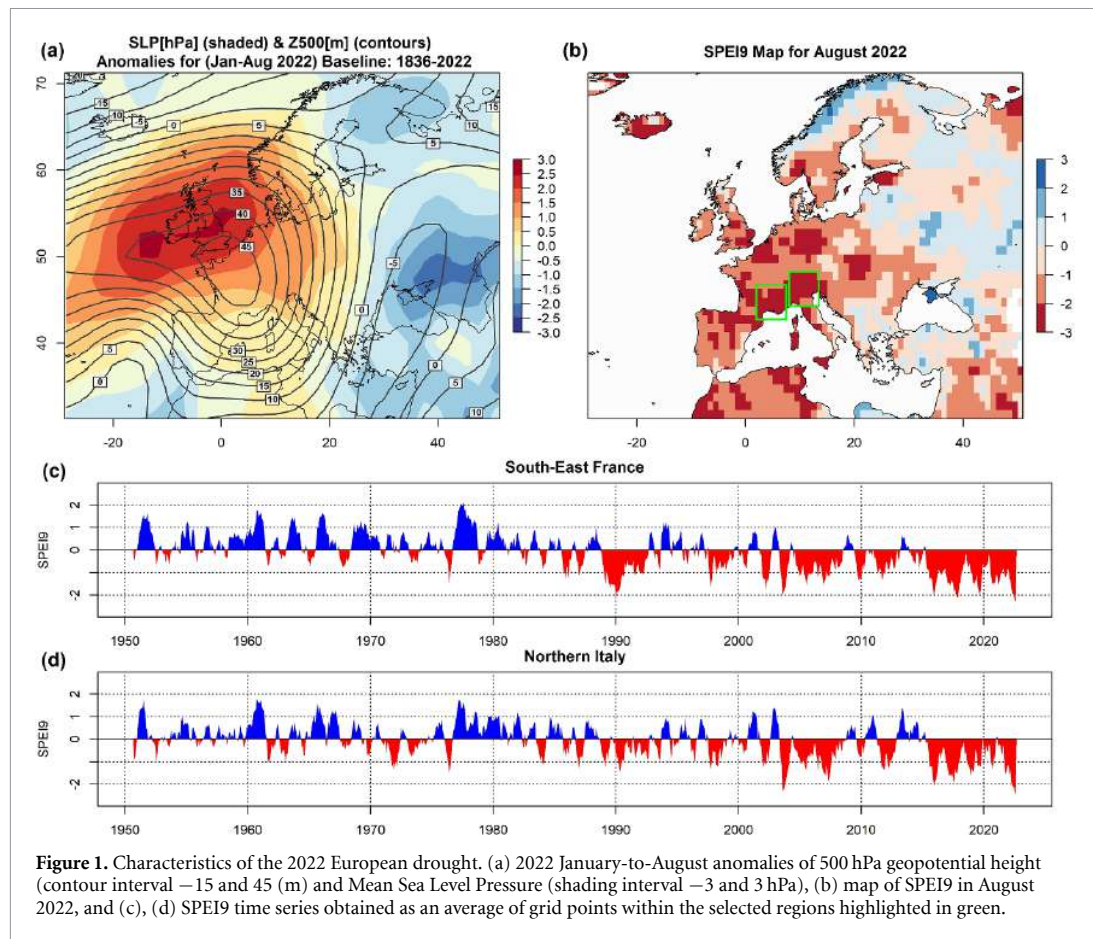
The 2022 drought had large societal impacts rising the attention of the media at the national and international levels [3, 13–15] and putting water management high on the agenda of water managers and decision-makers. Questions on the role played by the ongoing anthropogenic climate change (ACC) on this drought, and eventually on future droughts, are therefore pressing in the media debate, and answers to these questions are urgent to manage future similar water crises. Specifically, the questions we ask here are: how rare was the prolonged atmospheric circulation anomaly that drove the 2022 drought situation? Was such anomaly changed in shape, intensity, and thermal structure because of ACC, thus exacerbating similar drought events?

In this study, we address these questions through the method of the analogs of circulation for extreme event attribution [16, 17]. We use the implementation developed by [18] for short-lived meteorological events of a few days of duration (e.g. cyclones, hot and cold spells, etc), which we adapt to account for long-lasting events such as droughts. For the construction of factual and counterfactual climate [19], we rely on long-term monthly reanalyses (1836 to present) that allow for the construction of robust statistics. We, therefore, compare analogs of this averaged circulation in factual (1836–1915) and counterfactual (1941–2021) periods and study the associated temperature, precipitation, and SPEI9, looking for statistically significant differences that can then be attributed to climate change. Other complementary approaches for event attribution of extreme drought rely on single model initial-condition large ensembles [20–22]. While a model ensemble approach allows for a clear separation of counterfactual vs factual climate, it still suffers from model biases that can limit the realism of the results. Therefore in this study, we focus on reanalysis only, planning to analyze models as a second step.

2. Methods and data

2.1. Drought and circulation variables

To capture the 2022 drought condition, we use the Standardized Precipitation Evapotranspiration Index [4, 5] aggregated at nine months (SPEI9) as the 9-month aggregation timescale roughly corresponds to the period of negative precipitation deficit observed over western Europe. The SPEI generalizes the Standard Precipitation Index (SPI, [23]) by taking into account surface temperature too through its effects on Potential Evapotranspiration. It has been demonstrated that high temperatures—typical of, e.g. heat waves—increase drought stress under precipitation shortages by dramatically increasing evapotranspiration [24]. The SPEI is calculated first



by estimating the difference between precipitation and potential evapotranspiration at the surface, which provides a simple measure of the water deficit or surplus, and then aggregating it at different time scales (SPEI1, SPEI3, SPEI6, etc). Similarly to the SPI, the time scale of accumulation of the water deficits (e.g. 3 months, 6 months, 12 months, etc) is very important for practical reasons, as it differentiates meteorological droughts—typically of a few months' duration—from hydrological droughts, emerging at longer timescales (six months or longer).

The large scale atmospheric circulation over the North Atlantic-European sector is investigated through the 500 hPa geopotential height (Z500) and sea level pressure (SLP). All Z500 and SLP data used in the analyses of the analogs of circulation (see section 2.3) are first detrended and then deseasonalized by subtracting, for each month, the 1836–2022 monthly average. Details on these applied procedures can be found in the Supplementary Material and in figure S2. For the circulation analogs defined through Z500 and SLP, we also monitor the corresponding 2 m temperature, precipitation and SPEI9. We use the 2 m temperature to keep track of the impact of global warming, and the precipitation rate and SPEI9 to further cross-check drought conditions. We do not apply

any preprocessing to 2 m temperature, the precipitation rate, and SPEI9. A list of the variables and their symbols, used in this study are shown in table S1.

2.2. Data

In order to characterize the 2022 drought event over Europe (figure 1) we use SPEI9 obtained from the SPEI Global Drought Monitor, freely available at <https://spei.csic.es/index.html> at $1^\circ \times 1^\circ$ horizontal resolution from 1950 to present. The SPEI Global Drought Monitor offers near real-time SPEI estimates at various temporal scales (SPEI1, SPEI3, etc) at the global scale, based on the NOAA NCEP CPC GHCN_CAMS gridded dataset for mean temperature and the Global Precipitation Climatology Centre for the monthly precipitation data.

To search for analogs of the 2022 atmospheric circulation over the North Atlantic-European sector, and their relationship to the drought, we use the NOAA-CIRES-DOE Twentieth Century Reanalysis, version 3 (20CRv3) [25]. 20CRv3 is the latest version of 20CR, and implements many substantial improvements relative to previous versions [26]. 20CRv3 reanalyses are created by assimilating only surface pressure values and using observed monthly sea ice and sea surface temperature distributions as

boundary conditions. Estimates of the uncertainty are obtained using 80 ensemble members, which is a specific characteristic of 20CRv3. The choice of 20CRv3—which spans the period 1836–2015 and it is available at $1^\circ \times 1^\circ$ horizontal resolution—is dictated by the need of having a century-long reanalysis product that can thus provide more reliable statistics with regards to rare events, as in the case of intense droughts, and a sufficient number of analogs of the atmospheric circulation anomaly associated with the 2022 drought. In order to cover the most recent years (i.e. 2016–2022), we complement 20CRv3 for the period January 2016–August 2022 with NCEP reanalysis [27]. We use both the NCEP/DOE and NCEP/NCAR reanalyses (table S1). 20CRv3 and NCEP Reanalysis data are freely available at <https://psl.noaa.gov/data/gridded>. In order to eliminate differences between 20CRv3 and NCEP reanalysis datasets, we applied a bias correction to the complementary period 2016–2022 where datasets are obtained from NCEP reanalysis. Details of how we combined the two datasets as well as how bias corrections are performed are provided in the Supplementary Material and in figure S3. SPEI9 is calculated for the combined reanalyses 20CRv3 and NCEP by using the R package SPEI9 [5]. This tool assumes a log-logistic probability distribution [4] calibrated for 20CRv3 using all available years. We used the Thornthwaite equation as the method for determining potential evapotranspiration to be consistent with observations (SPEI Global Drought Monitor).

We evaluate the effect of interannual and interdecadal variability on the 2022 drought and on past analog droughts using the Niño3.4 index for ENSO (1870–present) and the Atlantic Multidecadal Oscillation (AMO, 1850–present) monthly indices computed from the HadISST1 data—the same SST used in the 20CRv3 reanalysis—and retrieved from KNMI's climate explorer www.climexp.knmi.nl. Missing values are replaced by NaN and not counted in the analysis. We remark that NaN values represent only less or at most about 10% of the total data. In particular, the Niño3.4 index is as defined by [28] and the AMO index is computed as described in [29].

2.3. Analog attribution method

The attribution method we use here is described in detail in [18], where it has been applied and validated for daily SLP maps associated with a number of extreme events occurred in 2021. In this study, we modify this method, born to deal with extreme events of the duration of a few days, in order to apply it to slow-evolving extreme events like droughts, which can have a duration of several months. To isolate the slow-evolving component of the atmospheric circulation (figure 1(a)) and for consistency with SPEI9, we smooth Z500 and SLP by applying a nine-month backward moving average. We then search for analogs

of the SLP and Z500 anomalies observed in August 2022 (figure 1(a)) in the factual period 1941–2021 and compare them to the analogs in the counterfactual period 1836–1915. The choice of these two periods is motivated by the need of having sufficiently long samples to select good analogs, while keeping a separation between periods with low and high CO2 emissions. For each period, we examine all monthly averaged maps and select the best 29 analogs, i.e. the maps minimizing the Euclidean distance to the event map itself. The number of 29 corresponds approximately to the smallest 3% Euclidean distances in each subset of our data. We tested the extraction of 15 to 30 analogous maps, without finding qualitatively important differences in our results. For the factual period, as is customary in attribution studies, the event itself is suppressed. In addition, we prohibit the search for analogs in 2022.

Unlike attribution techniques based on a statistical analysis of meteorological variables, conditioning to specific atmospheric circulation patterns via analogs allows us to link attribution to the dynamics driving extreme events. In addition, the analogs method allows us to determine when a weather event is unprecedented because of an atmospheric circulation that has never been observed in the past, making it statistically impossible to say whether climate change has made the event more likely. To account for the possible influence of low-frequency modes of natural variability in explaining the differences between the two periods, we also consider the possible roles of ENSO and AMO.

Following [18], we introduce additional indicators that further support our interpretation of analog-based results (see detailed description in supplemental material section 3):

2.3.1. Analog quality Q

Q is the average Euclidean distance of a given circulation pattern from its closest 33 analogs. One can then compare Q associated with the extreme event to Q for each analog of the extreme event. If the value of Q for the extreme event belongs to the same distribution of the values of Q for the analogs, then the extreme event has good analogs. If instead the Q for the extreme event is larger than that of the analogs, then the extreme event is associated with a very unusual circulation pattern, and care must be taken in interpreting the results. Differences between the counterfactual and factual periods in the value of Q associated with the extreme event indicate whether the atmosphere is visiting states (analog) that are more or less similar to the map associated with the extreme.

2.3.2. Predictability Index D

Using dynamical systems theory [30–32], we can compute the local dimension D of each Z500 (SLP)

map [33, 34]. The local dimension is a proxy for the number of degrees of freedom of the field, meaning that the higher D , the more unpredictable the temporal evolution of the Z500 (SLP) maps will be [33, 35, 36]. If the dimension D of the extreme event analyzed is higher or lower than that of its analogs, then the extreme will be respectively less or more predictable than the closest dynamical situations identified in the data.

2.3.3. Persistence index Θ

Another quantity derived from dynamical systems theory is the persistence Θ of a given configuration [37]. Persistence estimates the number of subsequent months we are likely to observe a map that is an analog of the one under consideration.

2.3.4. Seasonality of analogs

We can count the number of analogs per each month to detect whether there has been a shift in circulation to months earlier or later in the season. This can have strong thermodynamic implications, for example, if a circulation leading to large positive temperature anomalies in early spring becomes more frequent later in the season when average temperatures are much higher.

We compute the analog quality, the predictability index and the persistence index, and their statistical distribution, for extreme events in the factual and counterfactual world. Similarly, we estimate the persistence of the analogs for the two periods.

2.4. Association with ENSO and AMO

To account for the effect of natural interannual and interdecadal variability, we extract from the entire time series of the ENSO and AMO indices only the values in correspondence of ‘analog’ months, for both the counterfactual and factual periods. If the two distributions—ENSO (AMO) during analogs in the counterfactual period and ENSO (AMO) during analogs in the factual period—do differ significantly, then it is not possible to exclude that thermodynamic or dynamic differences in the analogs are partly due to these modes of natural variability, rather than anthropogenic forcing. On the other hand, if it is not possible to reject the null hypothesis of equal distributions, observed changes in analogs cannot be due to these two modes of natural variability and hence are attributed to human activity. It is worth noting that such null hypothesis of no influence of natural variability is coherent with the view of [38].

To assess the significance of changes in factual vs. counterfactual distributions, we conduct in all cases a two-sided Cramér-von Mises test at the 0.05 significance level. If the p -value is smaller than 0.05, the null hypothesis ($H = 0$) that the two samples come from the same distribution can be rejected [39].

3. Results

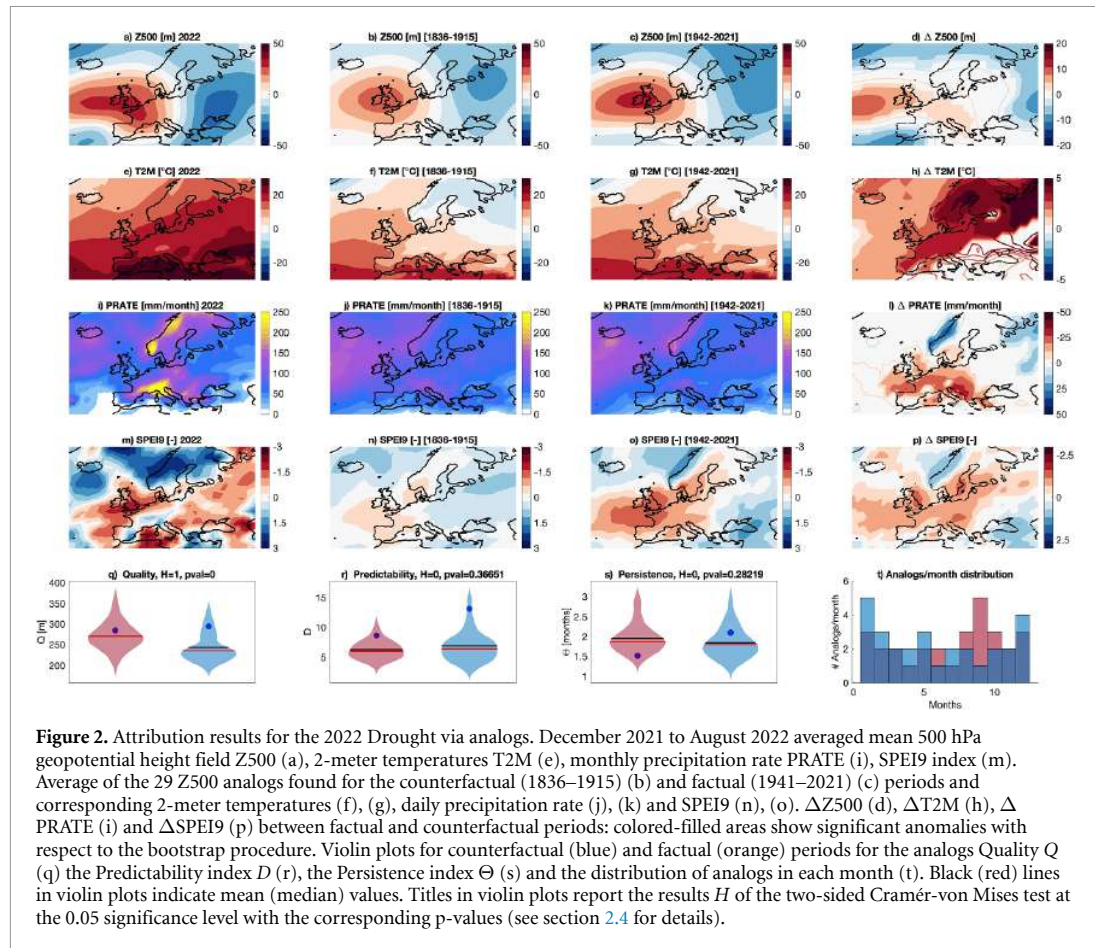
We perform the analogs attribution on both Z500 and SLP. Our results do not sensibly depend on the choice of the variable nor on the choice of applying or not the bias corrections to the reanalyses products (see Supplementary). Here we present the results for Z500 20CRv3 and DOE data with bias corrections, referring the reader for all other cases to the Supplementary Material.

3.1. Pattern analysis

Figure 2(a) shows the Z500 anomaly field averaged over the time period December 2021–August 2022. We note a dipolar structure of the Z500 anomaly, with positive values on Western Europe and negative on Eastern Europe, typical of Atlantic ridge patterns [40]. Analogs for the counterfactual (figure 2(b)) and factual (figure 2(c)) periods show a similar dipolar structure. The difference between the analogs of the factual and counterfactual period, $\Delta Z500$, highlights statistically significant diversities between the two fields (figure 2(d)). In particular, the factual climate features a dipole structure with larger positive anomalies over western Europe relative to the counterfactual climate. Furthermore, the positive anomaly has a larger spatial extension and it extends further westward over the Atlantic and southeastward towards the Mediterranean basin. This feature is pretty robust and independent of the choice of variables (SLP vs. Z500) and reanalyses (figures S4–S10).

Figure 2(e) shows T2M averaged over December 2021–August 2022 while figures 2(f) and (g) show the average T2M associated with the two sets of analogs. The analysis for T2M shows that the temperature field of the 2022 drought (figure 2(e)) is exceptionally warmer when compared to those associated with analogs of the counterfactual (figure 2(f)) or factual (figure 2(g)) periods. The difference $\Delta T2M$ between the two is shown in (figure 2(h)) and it shows an impressive warming associated with the Z500 analogs in the factual periods, as we would somewhat expect due to the ongoing global warming [41]. Note that this warming is way beyond the average global (1.2 °C) but also regional warming and does not include the event itself.

When comparing PRATE for the drought 2022 (figure 2(i)) with those associated with counterfactual (figure 2(j)) and factual (figure 2(k)) analogs, we note some similarities such as large precipitation amounts over the Alps, Norway, and southern Iceland, while the western Atlantic is dryer in 2022 than in the analogs. Let us bear in mind that these are precipitation estimates obtained from a reanalysis and therefore do not have to be considered as reliable as real observations. While not accurate, they are still useful



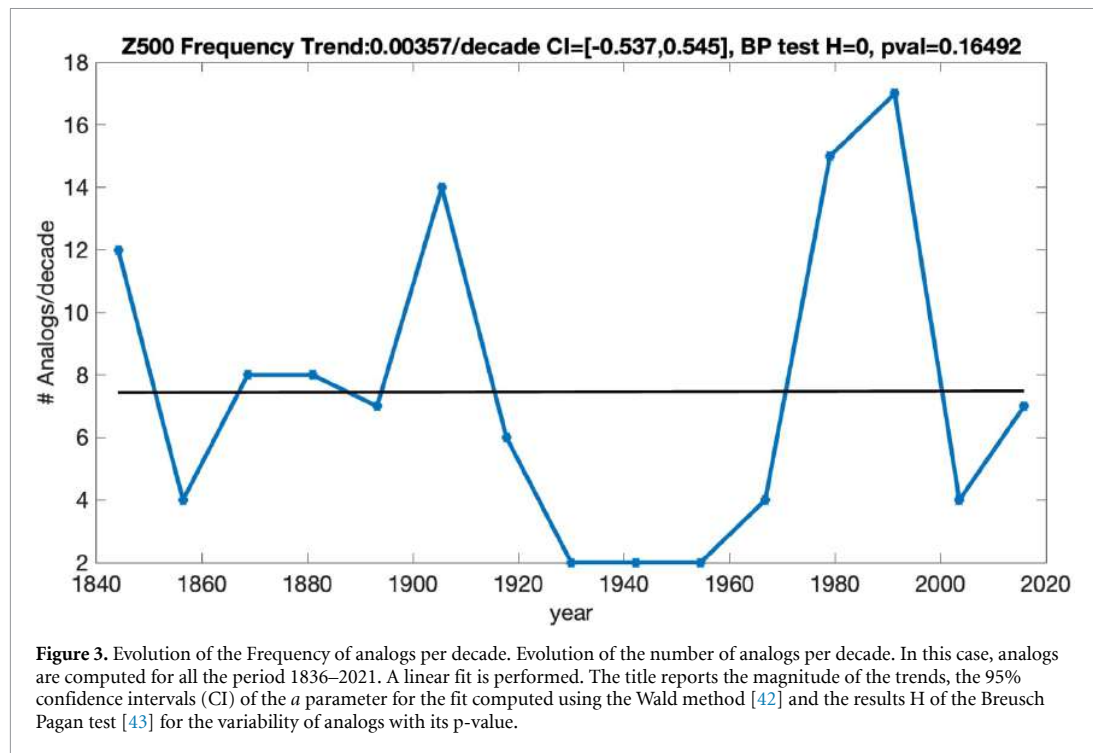
to connect circulation and thermal anomalies to precipitation deficits and hence droughts. What is more informative is the difference in PRATE associated with factual and counterfactual analogs (figure 2(l)), which shows a tendency to drier conditions in the factual climate relative to the counterfactual climate, with two minima over the British isles and over the Mediterranean.

We complete this analysis by comparing the pattern of SPEI9 of August 2022 (figure 2(m); see also figure 1(b) for an estimate of the same field based on observations) with the typical SPEI9 patterns associated with the Z500 factual and counterfactual analogs (figures 2(n)–(o)). When comparing the structure of SPEI9 from counterfactual to factual period (figure 2(p)), we see an extension of the area with negative values from Eastern Atlantic and the Iberian peninsula to all Western and Southern Europe. In fact, the resulting difference $\Delta SPEI9$ shows a marked tendency to negative values over all Europe. As SPEI9 takes into account both precipitation and surface potential evapotranspiration—which is temperature dependent—this patterns is fully consistent with both the tendency towards higher temperatures (figure 2(h)) and reduced precipitation (figure 2(l)) of Z500 analogs in the factual climate.

3.2. Dynamical indicators analysis

An analysis of the analogs quality Q (figure 2(q)) shows that factual analogs, as compared to counterfactual ones, are more similar to the Z500 pattern defined in figure 2(a). This is because the Euclidean distance of the 2022 circulation pattern from the factual analogs (blue dots) is well centered with the distribution of the distances of 2022 analogs from their analogs (pink violin plot). Contrary to that, the distance of the 2022 circulation pattern from the counterfactual analogs is at the edge for the counterfactual (blue violin plot). The difference between the distribution of the quality for the two periods is significant with p-value virtually zero. However, this is not consistent through the different members of the 20CRv3 ensemble (see section 3.5) so that these changes do not appear as robust.

The predictability (figure 2(r)) and the persistence (figure 2(s)) of the analogs do not show significant differences between the counterfactual and factual climates. The seasonality of the analogs (figure 2(t)) shows a tendency of observing such Z500 anomalies more in the summer and early autumn months in the factual period than in the counterfactual period. Supplementary figures S4–S10 show that this analysis is overall fairly qualitative insensitive to the choice of



the variable (Z500 or SLP) or the dataset or the bias-correction procedure employed, with the exception of the persistence of the analogs, which show a tendency to be more common in winter and spring in the factual climate when SLP is employed.

3.3. Frequency of occurrence

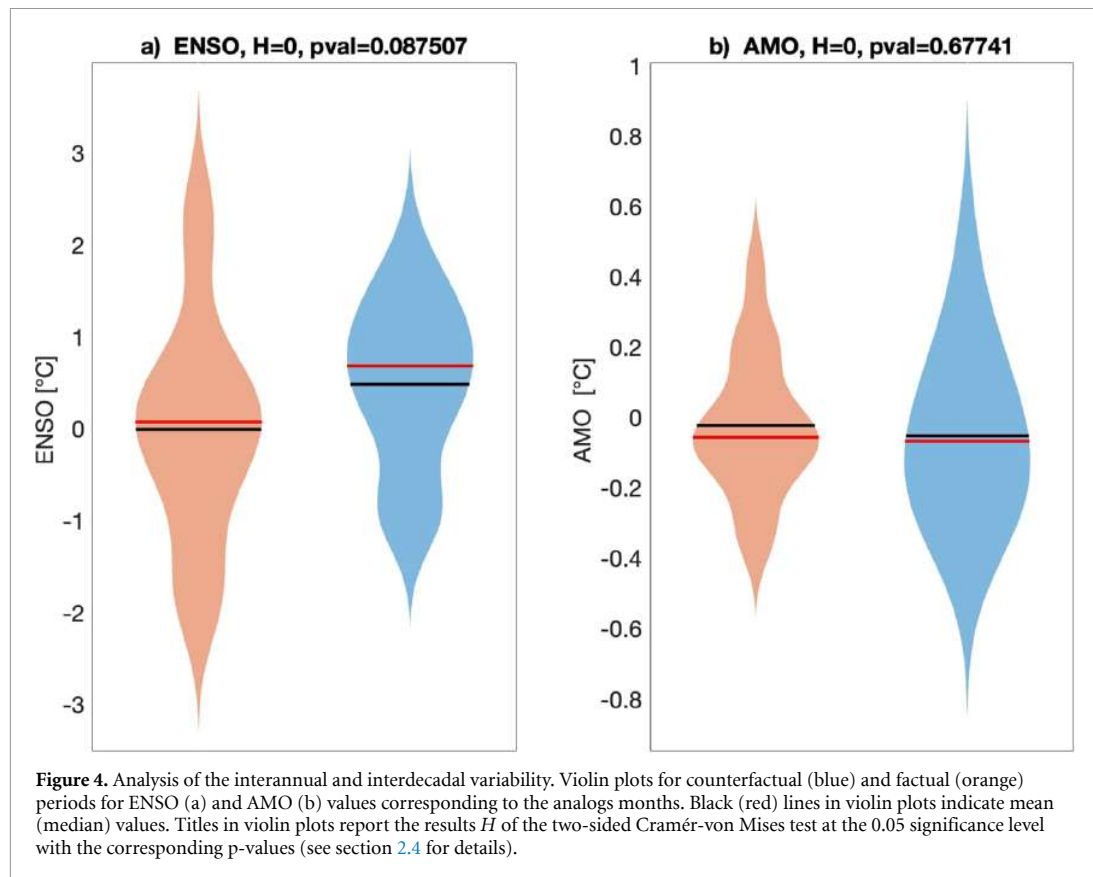
In order to determine whether the atmospheric circulation that led to the 2022 drought (figures 1(a) and 2(a)) has become more frequent in the factual climate, we now examine whether there is a trend in the frequency of the associated analogs over the whole 1836–2021 period, again leaving the year 2022 outside of this search. This analysis will allow us to isolate circulation trends on top of that induced by the thermodynamics, as we are using detrended SLP and Z500 data. For this analysis, we set the quantile for the analogs search to 0.95, i.e. we consider the 5% closest analogs to the event, to have enough analogs in each decade to estimate a robust trend. We have however tested trends obtained for higher quantiles (0.97, 0.98), i.e. looking at the 3% and 2% closest analogs without finding qualitative differences. Results are shown in figure 3, where we can see the number of analogs per decade. We estimate a linear trend $ax + b$ where x is the number of analogs per decade and the upper and lower 95% confidence intervals of the a parameter of the fit using the Wald method [42]. The analysis shows an increasing variability in the frequency of the analogs without any significant increasing or decreasing trends. Similar results are obtained for SLP and other datasets (figures S11–S17). This

leads us to conclude that the slow-evolving component of the circulation anomaly that drove the 2022 drought has not become more frequent in recent decades. Once the linear trend is removed, we investigate possible changes in the variability of the number of analogs using the Breusch-Pagan test [43] with a significance level 0.05. If the test statistic is found to be significant ($H = 1$, $pvalue < 0.05$), it suggests that the residuals are not homoscedastic: in our case, this would mean that the analogs' variability changes over time. We tested this hypothesis in our datasets: for the Z500 variables $H = 0$ in all cases (figures S11–S13) and for all the 80 ensemble members (table S2). For SLP only 15 members of the ensemble and the combination SLP bias corrected DOE (figure S14) is compatible with a change of variability in time.

3.4. Dependence on ENSO and AMO

Finally, we examine the association of the analogs with two major modes of interannual and interdecadal variability, namely ENSO and AMO. We build the probability distributions of the values of the ENSO and AMO indices selected at the months of the occurrence of analogs. If there exists a strong association between ENSO or AMO, and the circulation anomaly of figure 2(a), then we would find a probability distribution not centered around zero.

The results are shown in figure 4(a) for ENSO and in figure 4(b) for AMO. For the dataset used in the main text (20CRv3 plus NCEP/DOE) the analysis shows: (a) no significant changes in the distribution of ENSO (AMO) between the counterfactual



and factual world, and (b) no tendency for El Niño or La Niña (positive AMO or negative AMO) to prevail during periods characterized by circulation analogs of the one seen during December 2021–August 2022. That would seem to reinforce our initial conjecture (section 1) of no strong association between La Niña and the 2022 drought.

We note however that the p-value of the test for ENSO is equal to 0.088, close to the significance value of 0.05. Indeed some of the supplementary datasets shown in figures S18, S20 and S21 show a significant change in the distribution of ENSO between the counterfactual and factual climate. Hence, we cannot completely reject a moderate role of interannual variability in exacerbating the 2022 drought. Interestingly, the same analysis performed for the sea-level pressure patterns (figures S22–S24) show instead a dependence on the AMO but not on the ENSO.

3.5. Single-member analyses

The use of 20CRv3 reanalysis ensemble average at the beginning of the period can be problematic because it is based on a limited amount of observational data. This can lead to inaccuracies and biases in the ensemble average, which can affect the overall analysis. To address this issue, we repeated our analysis for all the 80 ensemble members. Results are

reported in Supplemental Material section 2, figures S25–S28 and table S2. This allows for a more comprehensive and accurate assessment of the data, as it takes into account the variability among the individual members. Results obtained for single members are largely consistent with those presented here for the ensemble means. The analysis of S25–S28 suggest that the standard deviation of the ensemble is way smaller than the averages, therefore the uncertainty in the reanalyses does not affect sensibly the results. Table S2 suggests that dynamical changes in predictability and persistence are more robust for SLP than Z500, and a prominent role of the AMO as sources of interdecadal variability. Only few members show changes in Analoqs Quality, so that the results found in figures 2 and S4–S10 (q) are specific of ensemble averages. For Predictability, Persistence and Variability, results of the ensemble are coherent with those of the ensemble means supporting our claim that analogs of our event have overall not changed significantly in time.

4. Discussion

We find a prominent role of the atmospheric circulation in driving the 2022 drought. There is a strong correspondence between the areas where Z500 was

higher in the 2022 and the anomaly of this quantity in the factual vs counterfactual period. In particular, the geopotential height is not just higher but the area with positive anomalies is also larger. As a consequence, while in the counterfactual periods droughts associated with these synoptic situations were confined to the British Isles, France, and partially the Iberian peninsula, in the factual world they embrace a larger portion of continental Europe and Italy. There is therefore a sort of ‘inflating balloon’ effect which expands the spatial extent of the drought and makes the anticyclonic dome higher, thus contributing to increasing the severity of the 2022 drought. This might be a ‘thermodynamic’ effect of global warming [44]. In addition to that, we also found that factual analogs get ‘warmer’, i.e. the near-surface temperature associated with them becomes higher (figure 2(h)). That leads to a more negative value of SPEI even if PRATE remains unchanged because higher surface temperature increases evapotranspiration, which dries the soil. This result is in line with [3], which focused on the exceptionality of the June–August soil moisture deficit in Europe and found that human-induced climate change made the 2022 root zone soil moisture drought about 3–4 times more likely, and the surface soil moisture drought about 5–6 times more likely.

While the ‘balloon’ expansion effect of Z500 is the most visible, we also note a change in the shape of the anticyclonic structure going from the counterfactual and factual periods, with the positive Z500 anomaly featuring a ‘crescent’ shape from the Atlantic through Central Europe into the Mediterranean (figure 2(d)). While this change in shape is of dynamical nature and thus related to systematic changes in the atmospheric circulation goes beyond the scope of this study, but would deserve further attention in future studies.

No trends in the frequency of this pattern have been observed and we do not have enough elements pointing to a change in the variability of the analogs with time. Finally, the analysis of the interannual and interdecadal oceanic variability on the 2022 drought suggests that we cannot completely rule out the influence of ENSO for the upper-level circulation and for the Atlantic Multi-decadal Oscillation for the lower-level circulation, although such influences are likely to be very modest.

5. Conclusions

According to the World Meteorological Organization, drought represents one of the most damaging and life-threatening climate-related hazards [45]. The attribution of drought events to human-caused climate change is not as clear as for other types of weather hazards like, e.g. heatwaves, because of the confounding role of natural variability [19]. Exceptional droughts have in fact occurred over the last two thousand years in association with decadal

variations in sea surface temperatures [46]. While the last IPCC 6th Assessment Report states that we have ‘medium confidence’ in attributing to human-induced climate change the increases in agricultural and ecological droughts because of increased land evapotranspiration [41, 47, 48], attribution to human-caused climate change of meteorological droughts—directly related to rainfall deficits and hence to atmospheric dynamics—remains challenging. Nevertheless, progress has been made and recent research highlighted the role of global warming in the exacerbation of some recent extraordinary meteorological droughts [20, 21, 49, 50].

In this study we considered the 2022 European-Mediterranean drought [1, 2] and investigated the exceptionality of the event and of its atmospheric drivers in a century-long reanalysis (1836–2021) using the analog-based methodology proposed in [18]. Our results indicate a role for ACC in making the atmospheric anticyclonic anomaly ‘stronger’ and ‘warmer’, two facts that in turn caused more widespread and exacerbated drought conditions. Conversely, we found that the frequency of occurrence of such a slow-evolving circulation component has not significantly changed over the last two centuries. These conclusions highlight a thermodynamic component in the exacerbation of droughts by human-caused global warming, while no strong evidence was found about a dynamical component—i.e. a change in circulation—in the recent period which could have triggered the 2022 drought.

While our study heavily relies on the observational datasets used and does not employ climate models, our results appear robust to the choice of meteorological variables and reanalysis. They further illustrate the capability of a reanalysis-based attribution conditioned on the atmospheric circulation on longer time-scales suggesting that this methodology could also be used to investigate other long-lasting events driven by synoptic situations such as prolonged cold periods or heatwaves.

An approach based only on atmospheric reanalysis, like the one applied in this study, while providing important information on the likelihood of the 2022 drought, has some limitations for attributing this extreme event to human-caused climate change, that is, first, the impossibility to define a counterfactual climate with no anthropogenic forcing and, second, the limited number of years available in reanalyses datasets. In a follow-up study thus we plan to complement this study by applying this method to climate models too, and in particular to single model initial-condition large ensembles [20, 51–54]. While these models are affected by systematic biases which can compromise their realism, they allow for a more rigorous definition of factual and counterfactual climate, and provide thousands of years of data is available for more robust statistics.

Data availability statement

The data that support the findings of this study are openly available at <https://psl.noaa.gov/data/gridded/>, <https://climexp.knmi.nl> and <https://spei.csic.es/map/>. The data generated and/or analyzed during the current study are available from the corresponding author on request.

Acknowledgments

D F received support from the European Union's Horizon 2020 research and innovation programme under Grant Agreement No. 101003469 (XAIDA) and the Marie Skłodowska-Curie Grant Agreement No. 956396 (EDIPI).

Author Contributions

S P devised the study, D F performed the analyses and B B prepared the datasets and performed the bias corrections. All authors contributed to discussing and writing the paper.

Conflict of interest

The authors declare no competing interests nor conflicts of interest. No human or animal data have been used in this study.

ORCID iDs

Davide Faranda  <https://orcid.org/0000-0001-5001-5698>

Salvatore Pascale  <https://orcid.org/0000-0002-6762-3283>

Burak Bulut  <https://orcid.org/0000-0003-4567-5258>

References

- [1] Toreti A et al 2022 Drought in northern Italy March 2022 (Luxembourg: Publications Office of the European Union) (<https://doi.org/10.2760/781876>)
- [2] Toreti A et al 2022 Drought in Europe August 2022 (Luxembourg: Publications Office of the European Union) (<https://doi.org/10.2760/264241>)
- [3] Schumacher D L et al 2022 High temperatures exacerbated by climate change made 2022 Northern Hemisphere droughts more likely WWA: *World Weather Attribution*
- [4] Vicente-Serrano S, Beguería S and López-Moreno J I 2010 *J. Clim.* **23** 1696–718
- [5] Beguería S, Vicente-Serrano S, Reig F and Latorre B 2014 *Int. J. Climatol.* **34** 3001–23
- [6] Baruth B et al 2022 *JRC MARS Bulletin* vol 30 (available at: <https://ec.europa.eu/jrc/en/mars/bulletins>)
- [7] Mishra A K and Singh V P 2010 *J. Hydrol.* **391** 202–16
- [8] Afshar M, Bulut B, Duzenli E, Amjad M and Yilmaz M 2022 *Agric. Forest Meteorol.* **316** 108848
- [9] Miralles D, Gentile P, Seneviratne S I and Teuling A J 2019 *Ann. New York Acad. Sci.* **1436** 19–35
- [10] Brönnimann S, Xoplaki E, Casty C, Pauling A and Luterbacher J 2007 *Clim. Dyn.* **28** 181–97
- [11] Brönnimann S 2007 *Rev. Geophys.* **45** RG3003
- [12] López-Parages J, Rodríguez-Fonseca B, Dommenget D and Frauen C 2016 *Clim. Dyn.* **47** 2071–84
- [13] Reuters 2022 Italy declares state of emergency for drought-stricken north (available at: www.reuters.com/world/europe/italy-declares-state-emergency-drought-stricken-north-2022-07-04/)
- [14] Bost A F, Villeneuve A, Armand M, Zabalza F, Gauchard Y, Foucart S and Rof G 2022 Drought in France: Tensions rise as rivers run dry *Le Monde* (available at: www.lemonde.fr/en/environment/article/2022/08/14/drought-in-france-tensions-rise-as-rivers-run-dry_5993566_114.html)
- [15] Kaleem J and Johnson S 2022 Los angeles times (available at: www.latimes.com/world-nation/story/2022-09-04/drought-europe-climate-change)
- [16] Yiou P, Jézéquel A, Naveau P, Otto F E L, Vautard R and Vrac M 2017 *Adv. Stat. Clim. Meteorol. Oceanogr.* **3** 17–31
- [17] Otto F E L 2017 *Annu. Rev. Environ. Resour.* **42** 627–46
- [18] Faranda D, Bourdin S, Ginesta M, Krouma M, Noyelle R, Pons F, Yiou P and Messori G 2022 *Weather Clim. Dyn.* **3** 1311–40
- [19] NAS 2016 *Natl Acad. Sci. Eng. Med.* **166**
- [20] Pascale S, Kapnick S, Delworth T L and Cooke W 2020 *Proc. Natl Acad. Sci. USA* **117** 29495–503
- [21] Pascale S, Kapnick S, Delworth T, Hidalgo H and Cooke W 2021 *Clim. Change* **168** 1–21
- [22] van der Wiel K, Lenderink G and de Vries H 2021 *Weather Clim. Extremes* **33** 100350
- [23] Hayes M, Wilhite D, Svoboda M and Vanyarkho O V 1999 *Bull. Am. Meteorol. Soc.* **80** 429–38
- [24] Adams H, Guardiola-Claramonte M, Barron-Gafford G A, Villegas J C, Breshears D D, Zou C B, Troch P A and Huxman T E 2009 *Proc. Natl Acad. Sci. USA* **106** 7063–6
- [25] Compo G P et al 2011 *Q. J. R. Meteorol. Soc.* **137** 1–28
- [26] Slivinski L C et al 2019 *Q. J. R. Meteorol. Soc.* **724** 2876–908
- [27] Kalnay E 1996 *Bull. Am. Meteorol. Soc.* **77** 437–72
- [28] Huang B, Thorne P W, Banzon V F, Boyer T, Chepurin G, Lawrimore J H, Menne M J, Smith T M, Vose R S and Zhang H M 2017 *J. Clim.* **30** 8179–205
- [29] Trenberth K E and Shea D J 2006 *Geophys. Res. Lett.* **33** RG3003
- [30] Freitas A C M, Freitas J M and Todd M 2011 *J. Stat. Phys.* **142** 108–26
- [31] Freitas A C M, Freitas J M and Vaienti S 2016 (arXiv:1605.06287)
- [32] Lucarini V, Faranda D, Freitas A C M, Freitas J M, Holland M, Kuna T, Nicol M, Todd M and Vaienti S 2016 *Extremes and Recurrence in Dynamical Systems* (New York: Wiley)
- [33] Faranda D, Messori G and Yiou P 2017 *Sci. Rep.* **7** 41278
- [34] Faranda D, Messori G and Vannitsem S 2019 *Tellus A: Dynamic Meteorology and Oceanography* **71** 1–11
- [35] Messori G, Caballero R and Faranda D 2017 *Geophys. Res. Lett.* **44** 3346–54
- [36] Hochman A, Alpert P, Harpaz T, Saaroni H and Messori G 2019 *Sci. Adv.* **5** eaau0936
- [37] Faranda D, Vrac M, Yiou P, Jézéquel A and Thao S 2020 *Geophys. Res. Lett.* **47** e2020GL088002
- [38] Trenberth K E 2011 Attribution of climate variations and trends to human influences and natural variability *WIREs Clim. Change* **2** 925–30
- [39] Anderson T W 1962 *Ann. Math. Stat.* **33** 1148–59
- [40] Dorrington J, Strommen K and Fabiano F 2022 *Weather Clim. Dyn.* **3** 505–33
- [41] IPCC 2021 *Summary for Policymakers. In: Climate Change 2021: The Physical Science Basis. Contribution of Working Group I to the Sixth Assessment Report of the Intergovernmental Panel on Climate Change* ed V Masson-Delmotte et al (Cambridge: Cambridge University Press) pp 3–32
- [42] Stein C and Wald A 1947 *Ann. Math. Stat.* **18** 427–33
- [43] Breusch T S and Pagan A R 1980 *Rev. Econ. Stud.* **47** 239–53
- [44] Faranda D, Vrac M, Yiou P, Jézéquel A and Thao S 2020 *Geophys. Res. Lett.* **47** e2020GL088002

- [45] World Meteorological Organization 2021 Weather-related disasters increase over past 50 years, causing more damage but fewer deaths (available at: <https://public.wmo.int/en/media/press-release/weather-related-disasters-increase-over-past-50-years-causing-more-damage-fewer>)
- [46] Cook B I *et al* 2022 *Nat. Rev. Earth Environ.* **3** 741–57
- [47] Herrera D A, Ault T R, Fasullo J T, Coats S J, Carrillo C M, Cook B I and Williams A P 2018 *Geophys. Res. Lett.* **45** 10619–26
- [48] Seneviratne S *et al* 2021 *Weather and Climate Extreme Events in a Changing Climate. In Climate Change 2021: The Physical Science Basis. Contribution of Working Group I to the Sixth Assessment Report of the Intergovernmental Panel on Climate Change*
- [49] Fischer E M, Seneviratne S I, Lüthi D and Schär C 2007 *Geophys. Res. Lett.* **34** L05707
- [50] Otto F E L *et al* 2018 *Environ. Res. Lett.* **13** 124010
- [51] Lehner F, Coats S, Stocker T F, Pendergrass A G, Sanderson B M, Raible C C and Smerdon J E 2017 *Geophys. Res. Lett.* **44** 7419–28
- [52] Deser C, Lehner F, Rodgers K B, Ault T, Delworth T L, DiNezio P N, Fiore A, Frankignoul C, Fyfe J C and Horton D E 2020 *Nat. Clim. Change* **1–10**
- [53] Zscheischler J and Fischer E M 2020 *Weather Clim. Extremes* **29** 100270
- [54] Gessner C, Fischer E M, Beyerle U and Knutti R 2022 *Weather Clim. Extremes* **38** 100512